Nuclear structure beyond the neutron drip line: The lowest energy states in ^{9}He via their T = 5/2 isobaric analogs in ^{9}Li

E. Uberseder [a], G.V. Rogachev [a,*], V.Z. Goldberg [a], E. Koshchiy [a], B.T. Roeder [a], M. Alcorta [b], G. Chubarian [a], B. Davids [b], C. Fu [c], J. Hooker [a], H. Jayatissa [a], D. Melconian [a], R.E. Tribble [a]

[a] *Department of Physics & Astronomy and Cyclotron Institute, Texas A&M University, College Station, TX 77843, USA*
[b] *TRIUMF, Vancouver, Canada*
[c] *Shanghai Jiao Tong University, Shanghai, China*

ABSTRACT

The level structure of the very neutron rich and unbound ^{9}He nucleus has been the subject of significant experimental and theoretical study. Many recent works have claimed that the two lowest energy ^{9}He states exist with spins $J^\pi = 1/2^+$ and $J^\pi = 1/2^-$ and widths on the order of 100–200 keV. These findings cannot be reconciled with our contemporary understanding of nuclear structure. The present work is the first high-resolution study with low statistical uncertainty of the relevant excitation energy range in the ^{8}He+n system, performed via a search for the T = 5/2 isobaric analog states in ^{9}Li populated through ^{8}He+p elastic scattering. The present data show no indication of any narrow structures. Instead, we find evidence for a broad $J^\pi = 1/2^+$ state in ^{9}He located approximately 3 MeV above the neutron decay threshold.

© 2016 The Authors. Published by Elsevier B.V. This is an open access article under the CC BY license (http://creativecommons.org/licenses/by/4.0/). Funded by SCOAP^3.

The quest to understand the superheavy helium isotope ^{9}He has been both long and fascinating. Interest in ^{9}He originates from its unusual ratio of neutron (N) to proton (Z) numbers (N/Z = 3.5). The largest N to Z ratio (N/Z = 3) found among nucleon-bound isotopes belongs to the next heaviest helium isotope, ^{8}He. A rather unusual feature of ^{8}He is seen in its two-neutron separation energy, which is larger than in the less neutron rich isotope ^{6}He. The isotope ^{9}He, which is unstable to neutron decay, appears even more unusual. There has been significant experimental effort to determine the level structure of ^{9}He. A detailed history of ^{9}He experimental studies has been recently given by Al Kalanee et al. [1], and we will provide a brief overview of the current experimental and theoretical status with respect to the ground and the first excited states in ^{9}He, which are the main focus of this letter.

The first observation of ^{9}He via the ^{9}Be(π^-, π^+) reaction was reported in 1987 by Seth et al. [2] and its ground state was identified at 1.13 ± 0.10 MeV above the neutron decay threshold. Seth et al. [2] noted surprisingly good agreement between the energies of the peaks in the observed spectrum of π^+-mesons and the predictions of a shell model, attributing a $J^\pi = 1/2^-$ spin assignment to the 1.13 MeV peak. Shortly thereafter, the ^{9}He ground state

was populated using the ^{9}Be(^{13}C, ^{13}O) and ^{9}Be(^{14}C, ^{14}O) reactions [3–5] and its energy was revised to 1.27 ± 0.10 MeV. It appeared to be a narrow resonance with width of only 100 ± 60 keV [5]. The majority of the experimental studies made after Ref. [5] supported the presence of a narrow $J^\pi = 1/2^-$ level at 1.3 MeV [6–8,1]. However, none of these experiments had simultaneously high resolution (comparable to the 100 keV natural width of the proposed state) with appreciably low statistical uncertainty. The only investigation which argued against such a resonance was that of Golovkov et al. [9], where the d(^{8}He, p)^{9}He reaction was performed using ^{8}He beam to populate states in ^{9}He. However, the energy resolution (~0.8 MeV) in Ref. [9] could be considered as a major obstacle in observing the 0.1 MeV narrow state.

The narrow width of the $1/2^-$ state was in evident contradiction with the original expectations based on the conventional shell model, that this state is a single particle state with a valence neutron occupying the 1p1/2 orbital on top of the closed 1p3/2 sub-shell. Using simple potential model it is easy to show that the single particle p-state at 1.3 MeV should have a natural width in the vicinity of 1 MeV, which is one order of magnitude larger than the experimental value. While energy of the first $1/2^-$ state in ^{9}He with respect to the neutron decay threshold depends on the specific residual interaction used in the shell model calculations, the spectroscopic factor (SF) is less sensitive and only

varies in the range between 0.5 and 0.9 (with SF of 1 being a "perfect" single particle state). These conclusions were confirmed in recent state-of-the-art *ab initio* calculations, that start from realistic nucleon–nucleon interactions and 3N forces and directly calculate the widths of the states of interest [10]. The width of the first $1/2^-$ state in ^{9}He was studied as a function of energy above the neutron decay threshold in Ref. [10] and it was shown that if the state is at 1.3 MeV above the neutron threshold then its width is expected to be 1.2 MeV. A factor of 10 discrepancy between the *ab initio* prediction for the width of this state and the experimental value is unusual in view of the fact that the same calculations do a very good job predicting width of narrow states in this mass region. For example, the width of the ^{7}He ground state $(3/2^-)$ calculated in Ref. [10] is perfectly within error bars of the experimental value of 0.122(13) MeV as are the widths of the narrow (0.033(6) MeV) 3^+ state in ^{8}Li at 2.26 MeV. The width of 0.63 MeV was suggested for the first $1/2^-$ state in ^{9}He by the recent Continuum Shell Model calculations [11], another theoretical approach that is able to predict the natural width of the resonance directly and was shown to work well for the chain of helium isotopes. Therefore, currently there is no existing theoretical model able to explain the narrow width of the first $1/2^-$ state in ^{9}He at present. Naturally, this raises the question of why the structure of $1/2^-$ state in ^{9}He is so different from all available theoretical predictions.

An interesting development in the study of ^{9}He occurred in 2001. A study of the two-proton knock-out reaction from ^{11}Be [12] was the first to identify a state with $\ell = 0$ at an energy less than 0.2 MeV above the ^{8}He+n threshold as the new ground state of ^{9}He. Since then, the existence of the $\ell = 0$ resonance in ^{9}He and its actual excitation energy has been a subject of much debate. There is a huge variation of the results from near zero scattering length [7,8], consistent with no or at most a very weak $\ell = 0$ final state interaction, to scattering length -20 fm [9] corresponding to a strong resonance near the neutron decay threshold in ^{9}He. Recently the d(^{8}He,p)^{9}He reaction was studied again [1] at the SPIRAL facility. The observation of the ground $2s1/2$ state close to the neutron decay threshold 0.18 ± 0.085 MeV and $1p1/2$ state at 1.2 ± 0.1 MeV with a width in the range from 0 to 300 keV (with 130 keV giving the best fit) was reported. Moreover, the authors also obtained angular distributions, which supported the spin-parity assignments for the observed states as $J^\pi = 1/2^+$ and $J^\pi = 1/2^-$. Here again the conclusions were made based on rather limited counting statistics.

In contrast, a very recent theoretical work connecting states in ^{9}He to states in ^{10}He [13] argues that the $J^\pi = 1/2^+$ state cannot exist below 1.0 MeV (otherwise ^{10}He must be neutron-bound) relative to the neutron threshold and is likely located more than 1.8 MeV above the neutron decay threshold based on the current knowledge of ^{10}He spectrum [13]. From the discussion above it is clear that there is an obvious disagreement between some experimental data and our theoretical understanding of nuclear structure of this exotic helium isotope and the main goal of this letter is to provide high quality experimental data that can guide us in resolving this long-standing problem.

The exotic nature of ^{9}He makes it a very difficult nucleus to probe experimentally. While many previous studies have endeavored to directly access ^{9}He states, the work described in this Letter obtains spectroscopic information on ^{9}He by attempting to populate T = 5/2 isobaric analog states in ^{9}Li through proton elastic scattering from ^{8}He. Such a technique is advantageous due to the high cross section involved in resonant elastic scattering. Furthermore, s-wave states that are otherwise virtual in ^{8}He+n configurations appear as real resonances in ^{8}He+p due to the presence of the Coulomb barrier. This experimental idea has been explored previously by Rogachev et al. [14]. However, due to imperfect ex-
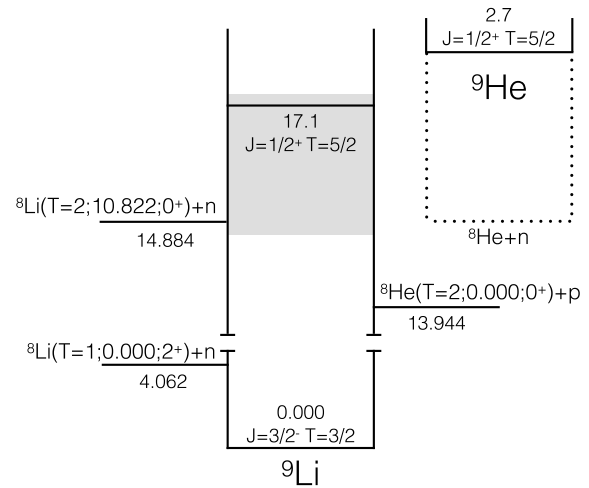

Fig. 1. Level diagram indicating the excitation energy of ^{9}Li probed in the current measurement (shaded region). The corresponding energies in ^{9}He are shown for comparison. All energies are in MeV. The decay thresholds are calculated from Refs. [19,20].

perimental conditions, analog states in ^{9}Li corresponding to low excitation energy in ^{9}He were inaccessible, and the energy resolution in the previous experiment [14] was too poor to observe an analog of the narrow $J^\pi = 1/2^-$ state. The authors of Ref. [14] did not observe it but verified that if the state is narrow ($\sim$100 keV) then its existence would not contradict the experimental data and that was considered as a confirmation of the narrow width of the $J^\pi = 1/2^-$ state in question.

The present work was performed with a ^{8}He beam and utilized the thick target inverse kinematics (TTIK) method [15–18], which has the advantage of measuring ^{8}He+p excitation functions for elastic scattering with a single beam energy. In this technique, the incoming ions are slowed in the target gas (methane) and the recoil protons are detected from a scattering event. These recoil protons emerge from the interaction with ^{8}He and hit Si detector array located at forward angles while the ^{8}He ions are stopped in the gas, as the protons have smaller energy losses than the scattered ions. Due to straggling effects, the energy and angular spread of the incoming ^{8}He ions increases as the ion traverses the scattering chamber. The spread of the beam in the chamber also depends upon its initial quality. Because we intended to populate the analog of the ground state in ^{9}He that may be unbound by only 200 keV or less, we needed to reach a ^{8}He+p center-of-momentum (CM) energy of about 1 MeV. Fig. 1 shows the corresponding neutron and proton thresholds in ^{9}Li. The excellent quality of the reaccelerated ^{8}He beam at the TRIUMF Isotope Separator and Accelerator (ISAC) facility, produced via the ISOL technique, enabled us to measure the ^{8}He+p elastic scattering cross section at much lower CM energies than has previously been possible [14] and with much better energy resolution on the order of 50 keV. The horizontal dotted line in Fig. 1 indicates the ^{9}He neutron decay threshold with respect to the excitation energy of the T = 5/2 isobaric analog states in ^{9}Li. It is important to note that the only neutron decay allowed by isospin conservation for these states is to the T = 2 excited state in ^{8}Li (isobaric analog of the ^{8}He ground state). In spite of its high excitation energy in ^{8}Li, the T = 2 state is very narrow (the upper limit is 12 keV); all decays by nucleons are forbidden due to isospin conservation. The shaded area in Fig. 1 represents the ^{9}Li excitation energy region studied in this experiment and demonstrates that the isobaric analogs of the states in ^{9}He that are barely unbound or even bound by few tens of keV would be populated in this experiment.
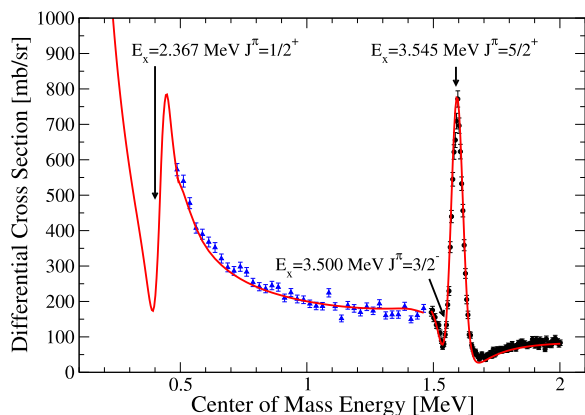
Fig. 2. The ^{12}C+p elastic scattering cross section measured with the present setup at TRIUMF (blue triangles) and TAMU (black circles). The red line is the R-matrix calculation (see text for the details). (To view this figure in color, the reader is referred to the online version of the article.)

The 32 MeV beam of ^{8}He ions with a 10^4 pps average intensity impinged on a scattering chamber filled with 990 Torr of methane gas, entering the chamber through a thin (4 μm) Havar film. A windowless ionization chamber (IC) was installed close to the entrance window to count (for normalization) and identify the incoming ions. The ^{8}He beam provided by ISAC was very pure; the only contaminant was ^{8}Li^{2+}, at a level of 2%, and was easily filtered using the IC. Three quadrant Si detectors (Micron Semiconductors MSQ25 type) were positioned symmetrically with respect to the beam axis at the distance of 513 mm from the entrance window, and provided information on the total energy of the recoil protons. A custom multi-anode position-sensitive proportional counter (MPPC) was installed in front of Si detectors to provide identification of the reaction products (using the ΔE-E technique) as well as their transverse position. A figure showing the particle identification can be found in the supplemental material [21]. Detailed Monte Carlo studies of the present setup indicate CM energy resolutions for ^{8}He+p elastic scattering events ranging from 40 keV full-width half-maximum (FWHM) at CM energy of 3 MeV to 100 keV at the lowest energy of 0.8 MeV for the forward Si detector.

By virtue of the experimental technique, any protons detected in the forward Si array are expected to arise from elastic scattering from ^{8}He. The primary sources of proton background in the present measurement would result from inelastic scattering and fusion evaporation. In both cases, the center of mass energies to make the reaction appreciable are such that the reactions occur at the entrance to the chamber. As low energy protons are expected from both reaction mechanisms, they do not have the energy to traverse the remainder of the gas and be detected in the silicon, and thus are effectively filtered in the present method. The fusion evaporation contribution has been modeled in detail, and supporting figures can be found in the supplemental material [22].

Measurements with ^{12}C beam were performed to test the experimental setup and to verify the analysis procedures. Fig. 2 shows the spectrum of protons from ^{12}C+p elastic scattering measured in two different runs. The lower energy data (blue triangles) were measured at the Cyclotron Institute at Texas A&M University (TAMU), and the higher energy data (black circles) were measured at the TRIUMF ISAC facility just before the ^{8}He main production run. The experimental setup was identical in all measurements. The red curve is an R-matrix calculation (not a fit), convoluted with experimental energy resolution. Parameters for the R-matrix calculations were obtained by fitting the differential cross sections of Meyer et al. [23] and are in perfect agreement with the known properties of the excited states in ^{13}N [24]. The agreement be-
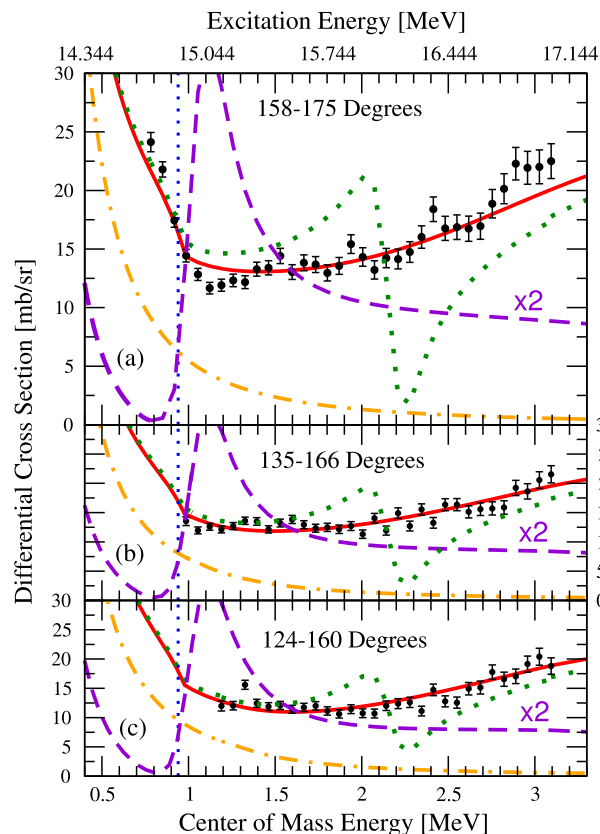

Fig. 3. ^{8}He+p elastic scattering excitation functions measured at three different lab. angles. The corresponding CM scattering angles are functions of energy with range shown for each section. The red solid curve is the best R-matrix fit. The orange dash-dotted curve is the Rutherford cross section. The green dotted curve demonstrates the sensitivity of these data to the hypothetical narrow T = 5/2 1/2$^-$ state in ^{9}Li. The purple dashed line shows the effect of a narrow T = 5/2 1/2$^+$ state in ^{9}Li (curve has been divided by two to appear on scale). The ^{8}Li(T = 2; E_x = 10.822 MeV; 0$^+$)+n threshold is shown as a dotted blue line. (To view this figure in color, the reader is referred to the online version of the article.)

tween the R-matrix calculations and the experimental data reflects the reliability of the analysis procedures.

Fig. 3 shows the excitation functions for ^{8}He+p elastic scattering obtained in the present measurement. The error bars indicate the statistical uncertainty. The individual spectra, from top to bottom, correspond to proton detection in the central detector, the inner halves of the outer detectors, and the outer halves of the outer detectors, respectively. Scattering events of varying energies take place at different distances from the detectors, and therefore at different laboratory angles. The corresponding average CM angles are shown for each spectrum in Fig. 3. The protons emitted with low energies at higher angle must traverse a longer path before reaching a Si detector and thus have greater energy loss to the gas. As such, the lower detection limit in CM energy increases from the top to the bottom plot.

There is a 1.5 MeV overlap region between these data and the data measured in the previous ^{8}He+p work [14]. The overall cross section is a factor of 1.5 higher in the new data set. We believe that this difference is due to the improved beam quality and the fact that the stopping location of the beam was much better defined in this experiment by using signals from the proportional counters. Also, there appears to be a minimum at 16 MeV excitation energy in Fig. 3 of Ref. [14]. This feature is clearly ruled out by the new measurement. The cross section is flat in this region and the previous minimum is shown to be a statistical fluctuation.
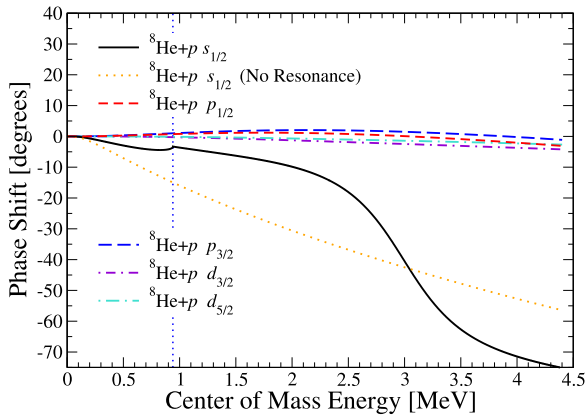
Fig. 4. The ^{8}He+p phase shifts for the various partial waves determined from the R-matrix fit to the ^{8}He+p excitation functions. All but the s-wave ($s_{1/2}$) phase shift, shown as the black solid curve, are featureless and close to zero at the measured energies. The pure potential model phase shift that does not include the broad T = 5/2 1/2$^+$ resonance is shown as the orange dotted curve. The ^{8}Li(T = 2; E_x = 10.822 MeV; 0$^+$)+n threshold is shown as a dotted blue line. (To view this figure in color, the reader is referred to the online version of the article.)

The spectra in Fig. 3 are rather featureless with the exception of a dramatic rise of the cross section at an energy corresponding to the ^{8}Li(T = 2; E_x = 10.822 MeV; 0$^+$)+n threshold, as seen in Fig. 3a. As demonstrated in Fig. 3, this rise cannot be explained by Rutherford scattering. The T = 3/2 levels in ^{9}Li in this excitation region are unknown, therefore a hybrid R-matrix approach based on the ideas of Refs. [25,26] was utilized in the analysis. In this approach the effect of the unknown T = 3/2 levels, which decay to many isospin-allowed open channels, is described by an optical model potential (details of the analysis will be published elsewhere). The introduction of the optical model increases the parameter space, though fortunately the $\ell = 0$ partial wave dominates the excitation function in the measured energy region ($kR \sim 1$), as expected from the nearly isotropic angular distributions. Contributions to the cross section from other partial waves were found to be negligible (see Fig. 4). The optical model potentials used in the present work should be considered phenomenological, as they were adjusted to minimize the R-matrix fit to the present data while varying the resonant T = 5/2 s-wave contribution. In spite of this, the present p-wave potential produces the ground state binding energy of ^{9}Li within 3 MeV.

The narrow $J^\pi = 1/2^-$ resonance, suggested to be at 1.3 MeV above the neutron decay threshold in ^{9}He [5,1], would have been easily observed in our data at an energy of about 1.2 MeV above the ^{8}Li(0$^+$, T = 2)+n threshold of 14.884 MeV. Instead, the excitation function in that energy region is featureless at all angles (Fig. 3). The manifestation of the $J^\pi = 1/2^-$ resonance with a 100 keV width in the energy region of interest is shown in Fig. 3 with green dotted curve. This calculation properly treated the neutron decay of the resonance to the ^{8}Li(T = 2; E_x = 10.822 MeV; 0$^+$), which is the dominant decay channel given that the neutron to proton (^{8}He+p) reduced width amplitude ratio is fixed by the isospin Clebsh–Gordon coefficients ($\gamma_n/\gamma_p = 2$). The experimental resolution is 50 keV at this CM energy and was also taken into account in the R-matrix calculation. To escape observation, the state would need to be as narrow as 20 keV in ^{9}He, i.e. even narrower than it was claimed in previous measurements. Another possible way this state could remain unobserved in the present measurement would be if it was strongly isospin impure. In this case the decays to many open T = 1 channels would make the resonance broader and weaker. Our calculations show that the isospin mixing would have to be nearly 50% to make this possible.

As stated above, the most natural explanation of the cross section rise near the ^{8}Li(T = 2; E_x = 10.822 MeV; 0$^+$)+n decay threshold is a manifestation of the Wigner cusp [27]. This decay threshold, located at an excitation energy of 14.9 MeV in ^{9}Li, is significant only for the T = 5/2 resonances. Closing of this channel leaves ^{8}He+p as the only open isospin-allowed decay channel for the T = 5/2 resonances and the cross section rises dramatically to preserve the incoming particle flux. To reproduce the threshold effect in question, a broad T = 5/2 $J^\pi = 1/2^+$ resonance needed to be introduced, with a width comparable to the distance between the resonance excitation energy and the ^{8}Li(T = 2; E_x = 10.822 MeV; 0$^+$)+n threshold. The actual parameters of the T = 5/2 $J^\pi = 1/2^+$ resonance are fairly sensitive to the shape of the observed cusp. The best fit (shown as a solid red curve in Fig. 3) is achieved with the $\gamma_p = 0.5$ MeV$^{1/2}$ and 17.1 MeV excitation energy for this state. The resulting s-wave phase shift, shown with the black solid curve in Fig. 4, clearly demonstrates the influence of the broad s-wave resonance on the behavior of the phase shift. It produces the sudden change of the phase shift derivative near the ^{8}Li(T = 2; E_x = 10.822 MeV; 0$^+$)+n decay threshold that is in turn responsible for the observed rise of the cross section. A low energy resonance with properties claimed in Ref. [1] is incompatible with the measured excitation function (see Fig. 3), as it leads to dramatic effects near the ^{8}Li(T = 2; E_x = 10.822 MeV; 0$^+$)+n decay threshold. The cross section near the resonance energy would be much higher than observed and would have a very distinct shape that is different from the experimental data (purple dashed curve in Fig. 3). Due to the upper limit of the data, it is difficult to state with certainty the energy of the T = 5/2 $J^\pi = 1/2^+$ state, other than to say that the c.m. energy is similar to the resonance width. Indeed, similar quality fits can be reproduced by pushing the state higher in energy and increasing the width and adjusting the s-wave optical potential. Conversely, a sharp rise in χ^2 is seen when forcing the state to lower energies. At an excitation in ^{9}Li of 16.8 MeV the value doubles from the minimum of $\chi^2 \approx 230$ ($\chi^2/N \approx 2.5$) regardless of width or potential adjustments, and we consider this to be a lower limit for the excitation energy for this broad T = 5/2 1/2$^+$ state in ^{9}Li.

Taking into account the shift functions of the ^{8}He+p and ^{8}He+n systems, the T = 5/2 $J^\pi = 1/2^+$ state physically appears in ^{9}He at c.m. energy of $\sim$3 MeV (with minimum of 2.3 MeV) above the neutron decay threshold with a width of $\sim$3 MeV (with minimum value of 2 MeV).

In summary, we report the first high resolution search with low statistical uncertainty for low-lying states in ^{9}He through their T = 5/2 isobaric analogs in ^{9}Li. We did not observe any narrow structures within the energy range of interest, and ruled out an existence of a narrow $J^\pi = 1/2^-$ state in ^{9}He. This conclusion is based on its absence in the T = 5/2 spectrum in ^{9}Li in the corresponding energy region. Given the good energy resolution ($\sim$50 keV) and high statistics of the ^{8}He+p data, the narrow T = 5/2 state can only be missed in our spectrum if its width is smaller than 20 keV or the isospin mixing is very strong ($\sim$50%). We consider both options as highly unlikely, but additional studies are certainly warranted. We also provided evidence for a very broad T = 5/2 state with spin $J^\pi = 1/2^+$ at an excitation energy of 17.1 MeV in ^{9}Li. This corresponds to a virtual broad ($\sim$3 MeV) state in ^{9}He at $\sim$3 MeV energy above the neutron decay threshold (with minimum energy of 2.3 MeV above the neutron decay threshold).

Two long-standing problems are resolved by these results. First, the mysterious discrepancy by a factor of 5–10 between the theoretical predictions and the experiment for the width of the low lying $J^\pi = 1/2^-$ state in ^{9}He has been eliminated by showing that there are no narrow resonances in ^{9}He at energies between 0 and

2.2 MeV above the neutron decay threshold (unless the two unlikely options mentioned above are realised). Second, it was shown that the actual energy of the $J^\pi = 1/2^+$ state in ^{9}He is far above that determined in Ref. [12] and more recently in Ref. [1] and that it has to be a very broad state. The important question remains: where is the first $1/2^-$ state and what is its width? It is not possible to give definitive answer to this question from the data presented in this Letter. The conservative statement is that the broad $T = 5/2$ $1/2^-$ state at excitation energy above the measured energy region in ^{9}Li (>17 MeV) cannot be excluded, but it was not necessary to introduce it to fit the experimental data.

Appendix A. Supplementary material

Supplementary material related to this article can be found online at http://dx.doi.org/10.1016/j.physletb.2016.01.014.

References

[1] T. Al Kalanee, J. Gibelin, P. Roussel-Chomaz, N. Keeley, D. Beaumel, Y. Blumenfeld, B. Fernandez-Dominguez, C. Force, L. Gaudefroy, A. Gillibert, J. Guillot, H. Iwasaki, S. Krupko, V. Lapoux, W. Mittig, X. Mougeot, L. Nalpas, E. Pollacco, K. Rusek, T. Roger, H. Savajols, N. de Sereville, S. Sidorchuk, D. Suzuki, I. Strojek, N.A. Orr, Phys. Rev. C 88 (2013) 034301.
[2] K.K. Seth, M. Artuso, D. Barlow, S. Iversen, M. Kaletka, H. Nann, B. Parker, R. Soundranayagam, Phys. Rev. Lett. 58 (1987) 1930.
[3] H.G. Bohlen, B. Gebauer, D. Kolbert, W. von Oertzen, E. Stiliaris, M. Wilpert, T. Wilpert, Z. Phys. A 330 (1988) 227.
[4] W. von Oertzen, H.G. Bohlen, B. Gebauer, M. von Lucke-Petsch, A.N. Ostrowski, C. Seyfert, T. Stolla, M. Wilpert, T. Wilpert, D.V. Alexandrov, A.A. Korsheninnikov, I. Mukha, A.A. Ogloblin, R. Kalpakchieva, Y.E. Penionzhkevich, S. Piskor, S.M. Grimes, T.N. Massey, Nucl. Phys. A 588 (1995) c129.
[5] H.G. Bohlen, A. Blazevic, B. Gebauer, W. von Oertzen, S. Thummerer, R. Kalpakchieva, S.M. Grimes, T.N. Massey, Prog. Part. Nucl. Phys. 42 (1999) 17.
[6] S. Fortier, E. Tryggestad, E. Rich, D. Beaumel, E. Becheva, Y. Blumenfeld, F. Delaunay, A. Drouart, A. Fomichev, N. Frascaria, S. Gales, L. Gaudefroy, A. Gillibert, J. Guillot, F. Hammache, K.W. Kemper, E. Khan, V. Lapoux, V. Lima, L. Nalpas, A. Obertelli, E.C. Pollacco, F. Skaza, U. Datta Pramanik, P. Roussel-Chomaz, D. Santonocito, J.A. Scarpaci, O. Sorlin, S.V. Stepantsov, G.M. Ter Akopian, R. Wolski, Search for resonances in ^{4}n, ^{7}H and ^{9}He via transfer reactions, in: AIP Conf. Proc., vol. 912, 2007, pp. 3–12.
[7] M.H. Al Falou, Etude de la structure des noyaux non liés ^{7,9}He et ^{10}Li, Ph.D. thesis, Université de Caen, 2007.
[8] H.T. Johansson, Y. Aksyutina, T. Aumann, K. Boretzky, M.J.G. Borge, A. Chatillon, L.V. Chulkov, D. Cortina-Gil, U. Datta Pramanik, H. Emling, C. Forssen, H.O.U. Fynbo, H. Geissel, G. Ickert, B. Jonson, R. Kulessa, C. Langer, M. Lantz, T. LeBleis, K. Mahata, M. Meister, G. Munzenberg, T. Nilsson, G. Nyman, R. Palit, S. Paschalis, W. Prokopowicz, R. Reifarth, A. Richter, K. Riisager, G. Schrieder, H. Simon, K. Summerer, O. Tengblad, H. Weick, M.V. Zhukov, Nucl. Phys. A 842 (2010) 15.
[9] M.S. Golovkov, L.V. Grigorenko, A.S. Fomichev, A.V. Gorshkov, V.A. Gorshkov, S.A. Krupko, Y.T. Oganessian, A.M. Rodin, S.I. Sidorchuk, R.S. Slepnev, S.V. Stepantsov, G.M. Ter-Akopian, R. Wolski, A.A. Korsheninnikov, E.Y. Nikolskii, V.A. Kuzmin, B.G. Novatskii, D.N. Stepanov, P. Roussel-Chomaz, W. Mittig, Phys. Rev. C 76 (2007) 021605.
[10] K. Nollet, Phys. Rev. C 86 (2012) 044330.
[11] A. Volya, V. Zelevinsky, Phys. At. Nucl. 77 (2013) 969.
[12] L. Chen, B. Blank, B.A. Brown, M. Chartier, A. Galonsky, P.G. Hansen, M. Thoennessen, Phys. Lett. B 505 (2001) 21.
[13] H. Fortune, Phys. Rev. C 91 (2015) 034306.
[14] G.V. Rogachev, V.Z. Goldberg, J.J. Kolata, G. Chubarian, D. Aleksandrov, A. Fomichev, M.S. Golovkov, Y.T. Oganessian, A. Rodin, B. Skorodumov, R.S. Slepnev, G. Ter-Akopian, W.H. Trzaska, R. Wolski, Phys. Rev. C 67 (2003) 041603.
[15] K. Artemov, O. Belyanin, A. Vetoshkin, R. Wolski, M. Golovkov, V. Goldberg, M. Madeja, V. Pankratov, I. Serikov, V. Timofeev, V. Shadrin, J. Szmider, Sov. J. Nucl. Phys. 52 (1990) 408.
[16] V. Goldberg, A. Pakhomov, Phys. At. Nucl. 56 (1993) 1993.
[17] V.Z. Goldberg, in: AIP Conf. Proc., vol. 455, 1998, pp. 319–322.
[18] G. Rogachev, E. Johnson, J. Mitchell, V. Goldberg, K. Kemper, I. Wiedenhover, Resonance scattering and α-transfer reactions for nuclear astrophysics, in: AIP Conf. Proc., vol. 1213, 2010, p. 137.
[19] G. Audi, A. Wapstra, C. Thibault, Nucl. Phys. A 729 (2003) 337–676.
[20] D.R. Tilley, J.H. Kelley, J.L. Godwin, D.J. Millener, J.E. Purcell, C.G. Sheu, H.R. Weller, Nucl. Phys. A 745 (2004) 155.
[21] See Supplemental Material at http://dx.doi.org/10.1016/j.physletb.2016.01.014 for particle identification plot.
[22] See Supplemental Material at http://dx.doi.org/10.1016/j.physletb.2016.01.014 for figures from a ^{12}C+^{8}He fusion evaporation simulation.
[23] H. Meyer, G. Plattner, I. Sick, Z. Phys. A 279 (1976) 41.
[24] F. Ajzenberg-Selove, Nucl. Phys. A 523 (1991) 1.
[25] D. Robson, Phys. Rev. 137 (1965) 535.
[26] W. Thompson, J. Adams, D. Robson, Phys. Rev. 173 (1968) 975.
[27] E. Wigner, Phys. Rev. 73 (1948) 1002.